Scilight

Low-Dimensional Materials
https://www.sciltp.com/journals/ldm

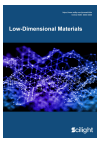

Review

Coherent Phonon Dynamics in 2D van der Waals Semiconductors

Xuchen Nie [1,*,†], Jiancheng Zheng [2,*,†] and Xiaoqiang Gao [3,*,†]

[1] Key Laboratory for Intelligent Nano Materials and Devices of Ministry of Education, State Key Laboratory of Mechanics and Control for Aerospace Structures, and Institute for Frontier Science, Nanjing University of Aeronautics and Astronautics, Nanjing 210016, China
[2] Fujian Key Lab of Agriculture IOT Application, College of Information Engineering, Sanming University, Sanming 365004, China
[3] Beijing Aerospace Institute for Metrology and Measurement Technology, Beijing 100076, China
* Correspondence: xcnie@nuaa.edu (X.N.); jczheng@fjsmu.edu.cn (J.Z.); 15811293752@163.com (X.G.)
† These authors contributed equally to this work.

How To Cite: Nie, X.; Zheng, J.; Gao, X. Coherent Phonon Dynamics in 2D van der Waals Semiconductors. *Low-Dimensional Materials* **2025**, *1*(1), 2.

Received: 6 August 2025
Revised: 19 September 2025
Accepted: 26 September 2025
Published: 16 October 2025

Abstract: Coherent phonon dynamics in two-dimensional (2D) van der Waals semiconductors represent an emergent frontier for controlling quantum states, energy transport, and optoelectronic functionalities through synchronized lattice vibrations. This comprehensive review synthesizes fundamental generation mechanisms, advanced ultrafast spectroscopy techniques, and material-specific manifestations across transition metal dichalcogenides (TMDs), magnetic semiconductors, perovskites, and related quantum materials. We establish how tailored phonon coherence enables unprecedented manipulation of electronic, optical, and spin states while highlighting persistent knowledge gaps and future research vectors for phonon-engineered quantum technologies.

Keywords: coherent phonon; ultrafast spectroscopy; 2D material

1. Introduction

Phonons, the quanta of lattice vibrations, are bosonic quasiparticles governing mechanical energy transfer in condensed matter systems. Analogous to photons in electromagnetic fields, phonons exhibit wave-particle duality and mediate critical interactions between charge, spin, and lattice degrees of freedom. While conventional phonon physics underpins thermal transport and structural stability, coherent phonon engineering has unveiled new paradigms for atomic-scale quantum control. Coherent phonons emerge when vibrational modes achieve phase synchronization across macroscopic dimensions, transforming stochastic thermal motions into deterministic quantum oscillations. Sustained over picosecond (ps)-to-nanosecond (ns) timescales, this collective coherence enables macroscopic quantum effects including phonon squeezing and photoinduced superconductivity. Critically, ultrafast optical excitation provides spatiotemporal control over these phase-locked oscillations, creating powerful avenues for dynamically tailoring material properties. Coherent phonons have now been extensively characterized in semimetals [1–6], semiconductors [7–10], superconductors [11–16], and topological insulators [17–19].

In atomically thin two-dimensional (2D) semiconductors (e.g. MoS_2, WSe_2, phosphorene), reduced dimensionality and weak dielectric screening amplify phonon-mediated phenomena while enabling band structure engineering through electron-phonon coupling, thermal transport regulation via selective phonon scattering, and light-matter interaction control via exciton-phonon correlations [20]. Such precise control over synchronized vibrations enables unprecedented manipulation of quantum states in atomically thin materials, bridging atomic-scale lattice motions to device-scale functionalities. Advancing this field requires experimental techniques with sub-picosecond resolution to elucidate ultrafast processes—carrier relaxation pathways, exciton formation mechanisms, and energy transfer dynamics. Notably, recent developments in ultrafast laser spectroscopy have revealed intricate couplings between electronic excitations and lattice vibrations in 2D systems. As a state-of-the-art characterization platform, ultrafast laser spectroscopy has proven essential for mapping transient states that critically determine operational performance in next-generation optoelectronic devices, ranging from high-efficiency photovoltaics to quantum photonic circuits and on-chip optical interconnects. Persistent challenges—including unresolved layer-dependent carrier lifetimes in transition metal dichalcogenides (TMDs) and divergent interpretations of phonon bottleneck mechanisms—highlight

critical knowledge gaps in quantum confinement and defect-mediated recombination dynamics, necessitating multidisciplinary approaches combining ultrafast spectroscopy, ab initio simulations, and defect engineering.

2. Generation Mechanism of Coherent Phonons

The coherent excitation of phonon displacement amplitude (Q) can be phenomenologically modeled as a damped harmonic oscillator driven by an impulsive driving force derived from femtosecond laser pulses. Mathematically, this driving term satisfies $\Delta t \ll 2\pi/\omega_0$, where Δt denotes the pulse temporal duration and ω_0 represents the phonon angular frequency. Fundamentally, this temporal constraint directly corresponds to a spectral requirement through Fourier transform duality: the pulse bandwidth $\Delta\omega$ must exceed ω_0. This requirement is rigorously dictated by the time-bandwidth product $\Delta t \cdot \omega_0 \geq K$, where K is a pulse-shape-dependent constant, typically ranging from 0.3 to 0.5. For instance, $K \approx 0.315$ for bandwidth-limited sech^2-shaped pulses and $K \approx 0.44$ for Gaussian pulses. Crucially, this dual time-frequency domain relationship establishes universal design criteria for coherent phonon manipulation in ultrafast spectroscopy techniques. The phenomenological equation of motion for the coherent phonon displacement amplitude Q, which can be derived from a quantum mechanical description [21], is expressed as [22,23]

$$\frac{d^2Q}{dt^2} + 2\Gamma\frac{dQ}{dt} + \omega_0^2 Q = F(t)/\mu \tag{1}$$

where Γ and ω_0 are the vibrational damping rate and frequency, respectively, $F(t)$ is the driving force exerted by the laser pulse, μ is the reduced lattice mass. The damping constant Γ is related to the dephasing time T_2 of the coherent mode via $\Gamma = 1/T_2$. This dephasing time T_2 is related to the population decay time T_1, which describes the decay of the diagonal terms of the density matrix via $2/T_2 = 1/T_1 + 1/T_p$, where T_p is the time related to pure phase-destroying processes [24]. Notably, the latter $1/T_p$ can be usually neglected for vibrational excitations in solids. Therefore, the observed dephasing time of a coherent phonon mainly reflects the population decay time; that is, time-domain measurements of T_2 via pump-probe techniques demonstrate quantitative agreement with frequency-domain determinations of T_1 through spontaneous Raman scattering linewidth analysis. For optical phonon modes, the population decay dynamics—neglecting electron-phonon interaction—arise predominantly from lattice anharmonicity, that is, high-frequency optical phonons dissipate energy by decaying into multiple low-energy acoustic phonon branches.

The generation mechanisms of coherent phonons are typically classified into two primary models. The first is impulsive stimulated Raman scattering (ISRS) [25,26], which occurs in transparent or opaque materials and is driven by an impulsive, δ-function-like force $F(t)$. The second is the displacive excitation of coherent phonons (DECP) [27–29], which is applicable to opaque materials and is driven by a step-function-like force $F(t)$. The operative mechanism in a given material depends on its optical properties. In transparent materials, the presence of only one Raman tensor means ISRS is the sole mechanism. In contrast, opaque materials possess two Raman tensors, which allows both DECP and ISRS to contribute and jointly determine the initial phase φ_0 [30].

2.1. Impulsive Stimulated Raman Scattering (ISRS)

A broadband optical pulse contains a spectrum of frequencies that enable multiple photon pairs (ω_1, ω_2) to satisfy the vibrational energy resonance condition ($\hbar\omega_1 - \hbar\omega_2 = \hbar\omega_0$, illustrated in Figure 1a). This generates an impulsive driving force to launch coherent nuclear motion on the ground electronic state, analogous to imparting an instantaneous kick to a pendulum's mass, initiating oscillatory motion. The critical requirements for ISRS are that the material must host Raman-active phonons (vibrational modes with nonzero Raman tensor components), and the pulse duration (Δt) must be shorter than the phonon period ($2\pi/\omega_0$) to ensure impulsive stimulation. The resultant nuclear displacement evolves sinusoidally over time. ISRS occurs under both nonresonant and resonant excitations. Under resonance, the Raman scattering cross-section is dramatically enhanced, leading to proportionally larger amplitudes of ISRS-driven coherent phonons.

2.2. Displacive Excitation of Coherent Phonon (DECP)

In DECP, coherent nuclear oscillations on the electronic excited state are triggered by a sudden shift in the equilibrium position of the vibrational potential. The displacement of the equilibrium coordinate $\Delta Q(t) = Q_0'(t) - Q_0$, scales linearly with the photoexcited carrier density $n(t)$, mirroring the abrupt translation of a pendulum's pivot point, which instantaneously alters its potential energy landscape (Figure 1b). Key requirements for DECP are such strong electron-phonon coupling (EPC) that shifts the potential energy surface by electronic excitation, and the pulse duration shorter than the phonon period. The resultant nuclear motion evolves as a cosine

function, distinct from the sine-phase oscillations in ISRS. This phase difference arises because DECP initiates vibrations through an abrupt displacement of the equilibrium position, whereas ISRS drives motion via an impulsive force (momentum transfer).

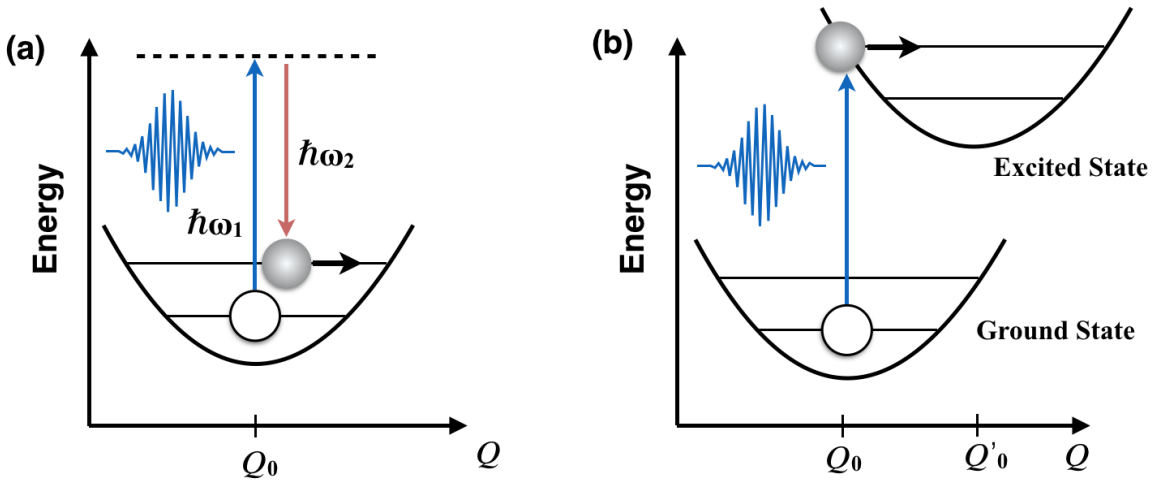

Figure 1. Two generation models of coherent optical phonons. (**a**) impulsive stimulated Raman scattering (ISRS). (**b**) displacive excitation of coherent phonons (DECP).

2.3. Experimental Verification of Coherent Phonon Generation Mechanism

The polarization dependence of pump excitation constitutes a critical experimental criterion for discriminating between the ISRS and DECP mechanisms. This fundamental distinction originates from their differential symmetry constraints. Coherent phonons generated via ISRS (a second-order nonlinear process) strictly follow the symmetry selection rules encoded in the Raman tensor $\chi^{(2)}$, thereby directly manifesting the material's intrinsic nonlinear optical susceptibility. In contrast, phonons induced by the DECP mechanism inherit the polarization dependence of optical absorption, as this process is governed by the momentum-selective electron-phonon coupling within the material's electronic band structure.

In certain systems, a single phonon mode may originate from both the ISRS and DECP mechanisms simultaneously. For such cases, the total polarization-dependent amplitude of the coherent phonon can be modeled as: $A(\theta) = A_{\mathrm{DECP}}(\theta) + A_{\mathrm{ISRS}}(\theta)$, where $A_{\mathrm{DECP}}(\theta)$ typically exhibits a $\cos^2(\theta)$-like dependence stemming from absorption anisotropy [31], and $A_{\mathrm{ISRS}}(\theta)$ varies according to the symmetry of $\chi^{(2)}$. By fitting the angular dependence of the phonon amplitude with appropriate symmetry-based functions, the relative contribution of each mechanism can be quantitatively determined.

These distinct polarization characteristics not only enable discrimination between generation mechanisms but also necessitate experimental techniques capable of resolving their ultrafast dynamics. The direct observation of coherent lattice vibrations—typically exhibiting picometer-scale amplitudes and lifetimes ranging from picoseconds to nanoseconds—requires exceptional temporal resolution and detection sensitivity. Ultrafast optical spectroscopy excels precisely in this regime, serving as the principal methodology for monitoring the entire temporal evolution of coherent phonons from their initial generation through subsequent dephasing and energy relaxation processes.

3. Ultrafast Optical Spectroscopy

Ultrafast optical spectroscopy has emerged as an indispensable analytical technique for probing non-equilibrium excited-state dynamics across multiple scales of matter. This methodology spans diverse physical systems, from isolated gas-phase atoms/molecules to complex condensed-phase architectures encompassing soft matter systems (e.g., proteins and lipid membranes) and hard crystalline solids. As a critical extension of conventional time-integrated optical spectroscopy, ultrafast optical spectroscopy provides unparalleled capabilities for deciphering the intricate non-equilibrium processes in low-dimensional semiconductor materials. Subpicosecond temporal resolution combined with spectral selectivity enables direct observation of fundamental quantum phenomena, including exciton-exciton coupling, electron-phonon coupling, coherent phonon dynamics, photoinduced phase transitions, and emergent quasiparticle formation dynamics [32]. These time-resolved investigations provide critical insights into the microscopic origins of macroscopic material properties, establishing ultrafast spectroscopy as a cornerstone technique in modern condensed matter physics and materials science.

The revolutionary development of ultrashort optical pulse technology over three decades has fundamentally

transformed experimental capabilities in non-equilibrium dynamics research. Through sustained innovations in mode-locked lasers and nonlinear frequency conversion techniques, researchers now achieve reliable generation and precise detection of sub-picosecond pulses spanning the terahertz (far-infrared) to hard *X*-ray spectral regimes. This paradigm-shifting advancement has enabled two complementary experimental approaches: (1) Low-fluence pump-probe spectroscopy for non-perturbative observation of intrinsic quantum dynamics; and (2) High-fluence excitation protocols for probing strongly-driven non-equilibrium states. The unprecedented access to ultrafast processes across this broad electromagnetic spectrum has established time-resolved spectroscopy as a universal tool for decoding multi-scale energy transfer pathways from molecular vibrations (THz) to electronic structure rearrangements (*X*-ray).

Ultrafast optical spectroscopy can be classified into transmission and reflection modes defined by their spatial geometries, each with distinct effective detection depths governed by the interaction of the probe light with the sample's optical and structural properties. In semiconductor research, the transmission mode is indispensable for interrogating bulk phenomena essential to charge generation, including excitonic dynamics and intrinsic recombination mechanisms, whereas the reflection mode enables the identification of surface and interfacial losses, such as trap states and interfacial charge transfer processes, which critically limit device performance. The synergistic application of these two modes provides complementary insights into both bulk and interfacial behaviors, thereby guiding the rational design of strategies to optimize the stability and operational efficiency of semiconductor-based devices. Formally, ultrafast optical spectroscopy is a nonlinear optical technique. In the low-fluence regime ($\leq 100\,\mu\mathrm{J/cm^2}$), pump-probe experiments can be described in terms of the third-order nonlinear susceptibility $\chi^{(3)}(\omega)$ [32, 33]. However, more insight is often obtained by considering ultrafast optical spectroscopy as a modulation spectroscopy where the self-referencing probe beam measures the induced change in reflectivity $\Delta R/R$ or transmission $\Delta T/T$ [34]. In general, the ultra-fast dynamic process in femtosecond pump-probe experiments can be understood as the dynamic modulation of the complex dielectric function $\tilde{\epsilon}(\omega) = \epsilon_1(\omega) + i\epsilon_2(\omega)$ or optical conductivity $\tilde{\sigma}(\omega)$ of a material by the photoexcitation, i.e. [34]

$$\Delta R/R(t) = \frac{\partial \ln(\mathrm{R})}{\partial \epsilon_1}\Delta\epsilon_1(t) + \frac{\partial \ln(\mathrm{R})}{\partial \epsilon_2}\Delta\epsilon_2(t) \tag{2}$$

where R is the reflectivity, and $\Delta\epsilon_1$, $\Delta\epsilon_2$ are the photoinduced changes in the real and imaginary parts of the dielectric function, respectively. In time-resolved optical reflectivity measurements, a first femtosecond (fs) laser pulse pumps the system into a non-equilibrium state, subsequently a relatively weaker laser pulse is implemented to probe the reflectivity change $\Delta R/R$, which is used to infer the intrinsic charge dynamics, based on the relation $\Delta R/R(t) = (\partial R/\partial n)n_{\mathrm{pe}} \propto n_{\mathrm{pe}}$ when the photoexcited quasiparticle density (n_{pe}) is small compared to the thermally excited one [35]. In the majority of experimental studies in condensed matter to date, the pump pulse creates a nonthermal electron distribution fast enough that, to first order, there is no coupling to other degrees of freedom. During the first 100 fs, the non-thermal (and potentially coherent) distribution relaxes primarily by electron-electron scattering. Subsequently, the excited Fermi-Dirac distribution thermalizes through coupling to the other degrees of freedom [36].

Over the past five decades, femtosecond transient absorption spectroscopy (fs-TAS) has emerged as a cornerstone technique in time-resolved spectroscopy, revolutionizing our understanding of ultrafast processes across multidisciplinary fields including photovoltaicss [37–41], photosynthetic mechanisms [42], and photochemical reactions [43–45]. Pioneered by Nobel laureate A. H. Zewail in foundational femtochemistry research [46], this technique achieved a historic milestone by resolving bond-breaking dynamics in iodine cyanide at femtosecond resolution. The evolution from conventional transient absorption spectroscopy to spatially resolved pump-probe microscopy (also termed transient absorption microscopy, TAM) [47–49] marks a transformative advancement in nonlinear optical imaging. By harnessing third-order nonlinear optical processes, this technique achieves exceptional spatiotemporal resolution to probe excited-state dynamics, facilitating novel investigations of functional materials and biological systems. Its integration of micron-scale spatial resolution with femtosecond temporal precision enables multidimensional mapping of excited-state relaxation pathways, nanoscale heterogeneity analysis in energy materials, and label-free identification of biopigments for diagnostic applications, thereby bridging critical gaps in both materials science and biomedical research. Notably, pump-probe microscopy surpasses conventional fluorescence-based methods by uniquely detecting non-radiative transitions in dark states, resolving chemical specificity for nonfluorescent chromophores, and achieving sub-diffraction-limit spatial resolution in optimized configurations, solidifying its role as an essential tool for nanomaterial photophysics research and precision bioimaging advancements.

4. Coherent Phonon in 2D Semiconductors

The precise excitation and manipulation of phonons represent longstanding objectives in condensed matter physics, electronics, and materials science [50–52]. Resonant ultrafast excitation of infrared-active phonon modes, enabled by femtosecond pump-probe spectroscopy (Figure 2), has emerged as a pivotal tool for dynamically controlling electronic states of complex materials that leads to remarkable phenomena such as light-enhanced superconductivity [53–57], light-induced transparency [58], transient ferroelectric polarization [59–63], non-equilibrium magnetization [64–68], and ultrafast insulator-to-metal phase transitions [10,69–73]. These phenomena arise from selective phonon-mode excitation, which modulates electron-electron and electron-lattice interactions at femtosecond timescales.

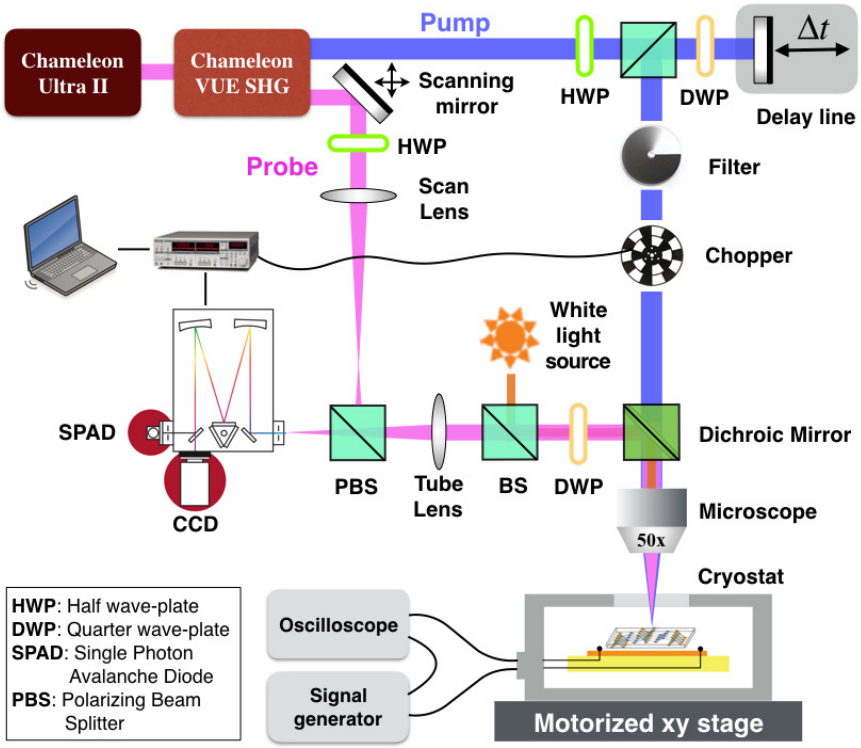

Figure 2. Schematic of femtosecond pump-probe system for coherent phonon spectroscopy. The probe beam path is designed with a $4f$ telescope system comprising three key components: (1) a motorized dual-axis galvanometer scanner with coplanar rotation axes aligned to the optical axis for high-precision beam steering; (2) a confocal plano-convex lens assembly that provides Fourier-plane relay imaging with integrated telecentric correction; and (3) a high-numerical-aperture microscope objective delivering uniform full-aperture illumination for diffraction-limited focusing performance. This optical configuration guarantees precise spatialtemporal overlap between pump and probe beams while maintaining exceptional wavefront fidelity across the entire scanning range.

Furthermore, coherent phonon states—characterized by phase-synchronized atomic displacements—can be generated in 2D materials via intense laser pulses or magnetically driven excitation mechanism. This capability offers novel pathways to tailor quantum coherence and symmetry-breaking processes [74–76], extending the impact of phonon engineering into low-dimensional systems.

The field of ultrafast control has expanded significantly since the pioneering work of Koshihara et al. [77] on photoinduced phase transitions. Ultrafast optical experiments are now routinely used to investigate a variety of nonequilibrium effects in quantum materials. Breakthrough results in the past decade include the surgical decoupling of microscopic degrees of freedom in iron-based superconductors [78–80], ultrafast switching into hidden phases in TMDs (e.g., $1T$-TaS_2) [81,82], dynamically controlled microscopic interactions in correlated transition-metal oxides [83], possible light-induced superconductivity in organic compounds K_3C_{60} [54], and photon-dressed (Floquet-engineered) topological states in materials like topological insulators (Bi_2Se_3) [84] and graphene, the latter marked by the emergence of photo-induced anomalous Hall effect [85]. Given this extensive context and the unique opportunities presented by low-dimensional systems, this article will next focus specifically on two-dimensional semiconductor materials.

4.1. 2D TMDs Semiconductors

TMDs have emerged as a revolutionary class of 2D semiconductors, exhibiting remarkable characteristics such as large exciton binding energies (hundreds of meV) and strong spin-valley coupling, which enable unprecedented control over light-matter interactions at the quantum level. The unique layer-dependent electronic structure of TMDs offers exceptional opportunities for optoelectronic engineering, as bulk and multilayer TMDs behave as indirect bandgap semiconductors, while their monolayer counterparts transition to direct bandgap systems (0.5–2 eV, tunable via composition and layer number) with dramatically enhanced photoluminescence efficiency. Quantum confinement in monolayers yields exceptional light absorption and robust room-temperature excitons. Combined with mechanical flexibility and silicon process compatibility, these properties enable groundbreaking applications such as ultra-sensitive photodetectors with superior gain performance, valleytronic devices exploiting quantum degrees of freedom, on-chip quantum light sources, and flexible wearable optoelectronics.

Resonant optical excitation of infrared-active lattice vibrations provides an effective means to induce targeted structural deformations in 2D TMDs semiconductors. Pioneering work in 2016 employed time-resolved transmission measurements to reveal coherent lattice vibration dynamics in mono- and few-layer WSe_2 flakes (Figure 3a) [86]. When monolayer WSe^2 was excited by ultrashort pulses resonant with its A-exciton transition, researchers observed the impulsive generation of coherent oscillations involving both the A_{1g} optical phonon and longitudinal acoustic phonon modes. Intriguingly, in multilayer WSe_2 systems, the interlayer breathing mode (B_1) exhibited a pronounced layer-number dependence, suggesting its utility as a sensitive spectroscopic probe for determining TMD thickness. Further investigations in monolayer $MoTe_2$ demonstrated that displacive excitation of A_{1g} phonons could dramatically modulate excitonic absorption characteristics (Figure 3b) [87], revealing exceptionally strong exciton-phonon coupling. Trovatello et al. also demonstrated strong phonon-exciton coupling in monolayer MoS_2, showing that its C excitons are strongly modulated by photoinduced coherent phonons [88]. Using transient absorption spectroscopy, they revealed enhanced phonon oscillations at exciton-phonon resonances, highlighting the interaction between out-of-plane phonon modes and excitonic states. This coupling becomes even more pronounced in carefully designed heterostructures, particularly due to interlayer charge separation effects in systems like $MoSe_2$/WSe_2 [75]. Remarkably, these heterostructures support a coherent 0.8 THz breathing mode that induces periodic modulation of both the van der Waals gap and interfacial electric field (Figure 3c). These studies demonstrate the rich diversity and tunability of phonon-exciton interactions in TMDs systems, providing fundamental insights into acoustic control of excitonic properties, a crucial advancement for next-generation optoelectronic device engineering. Conversely, the ability to coherently manipulate both intralayer and interlayer vibrations via optical excitation enables new paradigms for designing functional quantum materials with atomic-scale precision.

The intrinsic crystalline anisotropy in 2D materials, particularly in emerging TMDs such as $PdSe_2$ [89–91] and $PtSe_2$ [92,93] offers an additional degree of freedom for engineering electronic structures. As a novel member of the 2D TMDs family, $PdSe_2$ exhibits several exceptional properties such as high carrier mobility, thickness-dependent semiconductor-to-semimetal phase transition [90], and linear dichroism transition [89, 91]. The photocarrier dynamics in $PdSe_2$ show striking phase-dependent behavior. In the semiconducting phase (few-layer thickness), carrier relaxation is dominated by intraband hot-carrier cooling, interband recombination, and excitonic effects, all exhibiting minimal dependence on crystallographic orientation. In contrast, semimetallic (bulk) $PdSe_2$ displays strong orientation-dependent carrier relaxation dynamics governed by electron-phonon scattering (Figure 3d).

4.2. 2D Magnetic Semiconductors

In 2D magnetic semiconductors, such as CrSBr, $NiPS_3$ [94], and $FePS_3$, the coexistence of tightly bound excitons (with large oscillator strengths) and long-lived coherent magnons [95], enabled by narrow bandgaps and spatial confinement) creates a unique platform for spin-wave-mediated excitonic engineering. Here, the primary excitonic transitions can be dynamically modulated through the coupling between spin waves and electronic structures. Particularly in CrSBr, an antiferromagnetic semiconductor, there exists long-range propagating coherent magnon modes with propagation lengths exceeding 7 μm and coherence times surpassing 5 ns [66]. These coherent magnons persist in bilayer and multilayer configurations across compensated and uncompensated magnetic states, originating from strong coupling of Wannier exciton to interlayer magnetic order via spin-dependent interlayer electron-exchange interactions [96,97]. The intricate interplay among competing degrees of freedom in quantum systems underlies the emergence of exotic matter phases characterized by non-trivial order parameters and emergent collective excitations. Employing phase-resolved coherent phonon spectroscopy, N. Gedik's group has uncovered a mode-selective magnetoelastic effect in $FePS_3$, characterized by amplitude and phase modulation of the 7.51 THz coherent phonon mode [67]. It is of utmost importance that coherent phonon spectroscopy has been established as a highly sensitive method for detecting hidden spin-lattice interactions in van der Waals magnetic semiconductors and

other systems with strong spin-lattice coupling. Moreover, strong exciton-magnon coupling provided a new approach for regulating non-equilibrium magnetic phases through nonlinear phononics, or vice versa.

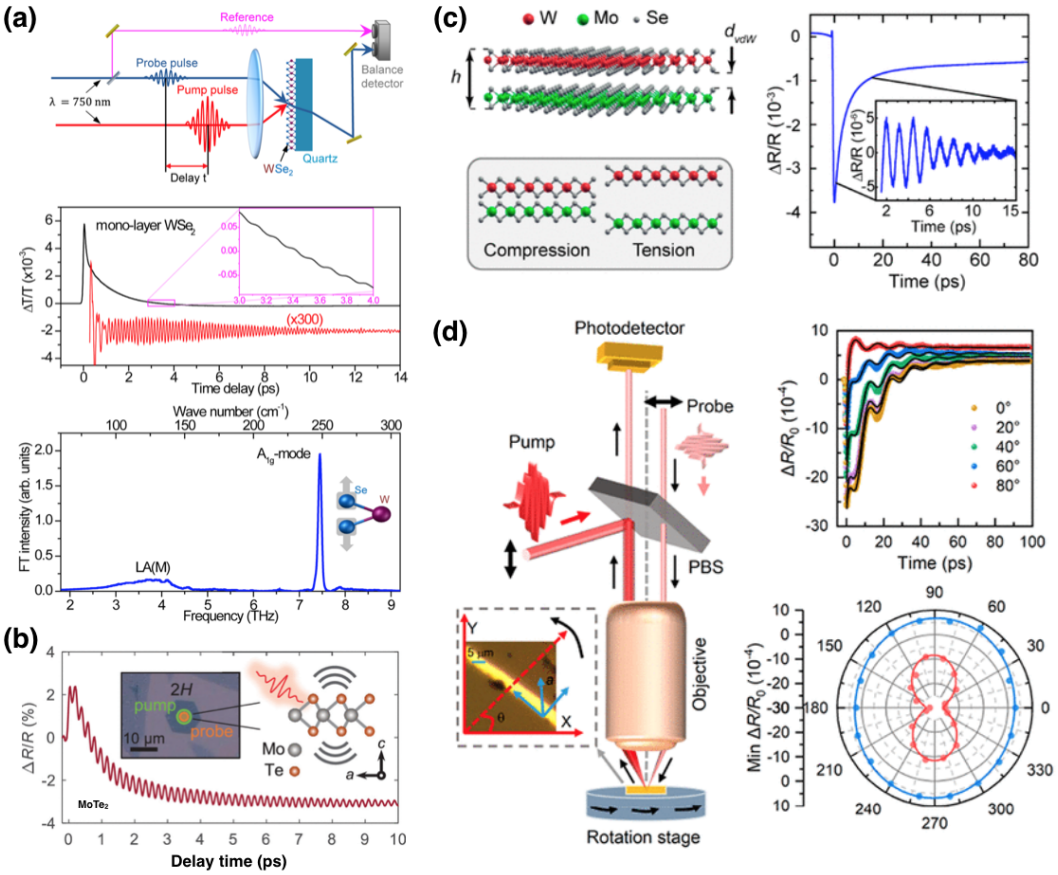

Figure 3. Coherent phonons in 2D TMDs semiconductors. (**a**) Coherent phonon detection in monolayer WSe_2 through transient transmission spectroscopy. Time-domain $\Delta T/T_0$ signal reveals coherent oscillations. Fourier transform spectrum identifies the out-of-plane A_{1g} optical phonon mode at 7.45 THz and a broad feature at ∼3.7 THz corresponding to the longitudinal acoustic phonon mode. Copyright 2016, American Chemical Society [86]. (**b**) Detecting coherent phonon from transient absorption microscopy in monolayer $MoTe_2$. Copyright 2023, American Chemical Society [87]. (**c**) Coherent interlayer breathing mode in $MoSe_2/WSe_2$ heterobilayers. The observed phonon mode periodically modulates the van der Waals gap spacing, effectively tuning the total heterostructure thickness at terahertz frequencies. Copyright 2023, American Chemical Society [75]. (**d**) Polarization-resolved transient reflectivity spectra of 16.4 nm-thick $PdSe_2$ ribbons. The $\Delta R/R_0$ values at t = 0 ps (red solid circles) exhibit clear two-fold rotational symmetry, indicative of anisotropic optical response in the material. Copyright 2024, American Chemical Society [89].

4.3. 2D Perovskite Semiconductors

Organic-inorganic hybrid layered perovskites demonstrate exceptional promise for optoelectronic applications including light-emitting diodes, lasers, photodetectors, and solar cells due to their large exciton binding energies, compositional flexibility, enhanced environmental stability, and structural homogeneity [98]. As direct bandgap semiconductors, they exhibit high absorption coefficients enabling the fabrication of thin films that effectively suppress bulk-phase defects, with grain boundary and interface defects further mitigated through passivation modifications [99]. Their uniquely prolonged hot-carrier relaxation dynamics enables transformative technologies such as high-efficiency hot-carrier photovoltaics, photocatalysis, and photodetectors [98,100,101].

Electron-phonon interactions fundamentally govern charge transport and transfer in these materials. In the prototypical 2D perovskite $(PEA)_2PbI_4$ (PEA = phenylethylammonium), distinct excitons exhibit varying coupling strengths with coherent phonons, inducing specific lattice reorganizations that reveal differential polaron characteristics [20, 102]. The 2D double perovskite $(AE2T)_2AgBiI_8$ (AE2T: 5,5″-diylbis(amino-ethyl)-(2,2″-(2)thiophene)) demonstrates how inorganic framework energy oscillations enable controllable hole transfer between organic and inorganic components [103], establishing electron-phonon coupling as an engineering strategy for manipulating charge transfer kinetics through coherent processes. Cross-plane coherent phonon dynamics have been systematically investigated via pump-probe spectroscopy [104,105]. Using probe wavelengths beyond the

optical bandgap minimizes attenuation, enabling deeper penetration and longer phonon lifetimes. Conversely, probing at the optical bandgap can further resolve structural heterogeneity influences. The heat-carrying longitudinal acoustic phonons propagating along the cross-plane direction of 2D Ruddlesden-Popper hybrid perovskites were experimentally observed in the near-infrared spectral region by Guo et al. [104]. Critically, phonon oscillation frequency and velocity exhibit a layer-number effect—decreasing with increasing inorganic layer count due to increased inorganic mass and reduced electron-phonon coupling [105]. Organic spacer chemistry significantly modulates vibrational relaxation dynamics as demonstrated by Quan et al. [106]. Flexible alkylamine spacers enable fast relaxation (∼0.3 ps) with negligible temperature dependence, while aromatic amine spacers exhibit moderate relaxation (∼1.2 ps) with significant thermal sensitivity. Ultrafast spectroscopy and molecular dynamics simulations attribute this to organic ligand-dependent variations in lattice anharmonicity and dynamic structural disorder governing optical phonon dephasing rates. Solvent engineering emerges as a critical control parameter for phonon modulation. Cui et al. [107] established that dimethyl sulfoxide (DMSO)-processed $(PEA)_2PbBr_4$ films exhibit three optical phonon modes (M1–M3), whereas N,N-dimethylformamfide (DMF)-processed counterparts show only two vibrational modes with the M3' mode red-shifted by 4.5 cm^{-1} relative to DMSO-M3. Femtosecond transient absorption spectra confirm solvent selection directly influences vibrational lifetimes, exciton-phonon coupling strength, and exciton resonance behavior, providing fundamental insights for tailoring perovskite phonon dynamics in next-generation optoelectronics. Future exploitation of coherent phonon dynamics via advanced ultrafast spectroscopy will unlock tailored exciton-phonon coupling control in 2D hybrid perovskites, enabling rationally designed high-efficiency photovoltaic and quantum optoelectronic devices.

4.4. Other Types of 2D Semiconductors

Black phosphorus (BP) is an emerging 2D semiconductor with unique layer-dependent electronic and optical properties [108], featuring a tunable direct bandgap that spans from 0.3 eV (bulk) to ∼2 eV (monolayer). Its puckered honeycomb lattice structure gives rise to remarkable anisotropic characteristics [109–113], manifesting as pronounced differences between the armchair (AC) and zigzag (ZZ) directions in optical, mechanical, and electrical properties. Using pump-probe microscopy with spectral-temporal resolution, Ji et al. observed layer-dependent transient absorption resonances in BP, attributed to bandgap renormalization from strong many-body interactions [108]. Their work revealed that ultrashort laser pulses can impulsively drive coherent atomic motions strongly coupled to electronic transitions, which correspond to the low-frequency layer-breathing mode (Figure 4a). Remarkably, they discovered coherent phonon oscillations with thickness dependence well explained by a linear chain model, enabling rapid phonon frequency mapping (Figure 4b–e). Most intriguingly, they observed π-phase-shifted coherent phonon oscillations between armchair and zigzag polarizations, revealing opposite photoelastic responses under longitudinal strain [112]. In addition, an anomalous coherent acoustic phonon mode with pressure softening behavior was observed within the range of ∼3–8 GPa, showing distinct pump fluence and time dependences [114]. These findings demonstrate BP's exceptional potential for developing ultrafast, polarization-sensitive optoelectronic and photoacoustic devices. Complementing these studies, Meng et al. utilized polarization-resolved transient absorption microscopy to study anisotropic charge carrier and phonon dynamics in BP [111]. Their results revealed polarization- and thickness-dependent carrier decay rates and phonon damping, attributed to BP's intrinsic refractive index anisotropy. Through analysis of the oscillation amplitude and phase, the group concluded that phonon generation was primarily governed by the direct deformation potential mechanism. Furthermore, they independently determined the sound velocity through both oscillation frequency and acoustic echo measurements, with the results showing excellent consistency. These comprehensive investigations provide crucial insights into BP's acoustic phonon properties and highlight its exceptional potential for polarization-sensitive optoelectronic and photoacoustic applications.

BiI_3 has recently gained significant attention as an environmentally friendly alternative to lead-based perovskites for optoelectronic applications, owing to its prominent excitonic features. The material exhibits a strong direct excitonic transition at 620 nm characterized by a nanosecond-scale lifetime and exceptional binding energy exceeding 200 meV. Fundamental studies using resonant Raman spectroscopy have revealed strong coupling between excitons and the dominant A_g-symmetry optical phonon mode at 3.4 THz. Advanced ultrafast spectroscopy techniques have provided deeper insights into these interactions. Transient absorption measurements on solution-processed BiI_3 thin films have captured the coherent dynamics of both A_g phonons and excitons following femtosecond photoexcitation [115]. Time-resolved broadband optical spectroscopy on BiI_3 single crystals has further established coherent phonon oscillations as unambiguous markers of exciton-phonon coupling in layered semiconductors [116]. These results establish sub-picometer resolution in mapping exciton-phonon interactions, uncovering new mechanisms for nonequilibrium control in 2D semiconductors where excitation fluence and resonance enable precise exciton engineering, and providing fundamental insights for designing quantum optoelectronic materials.

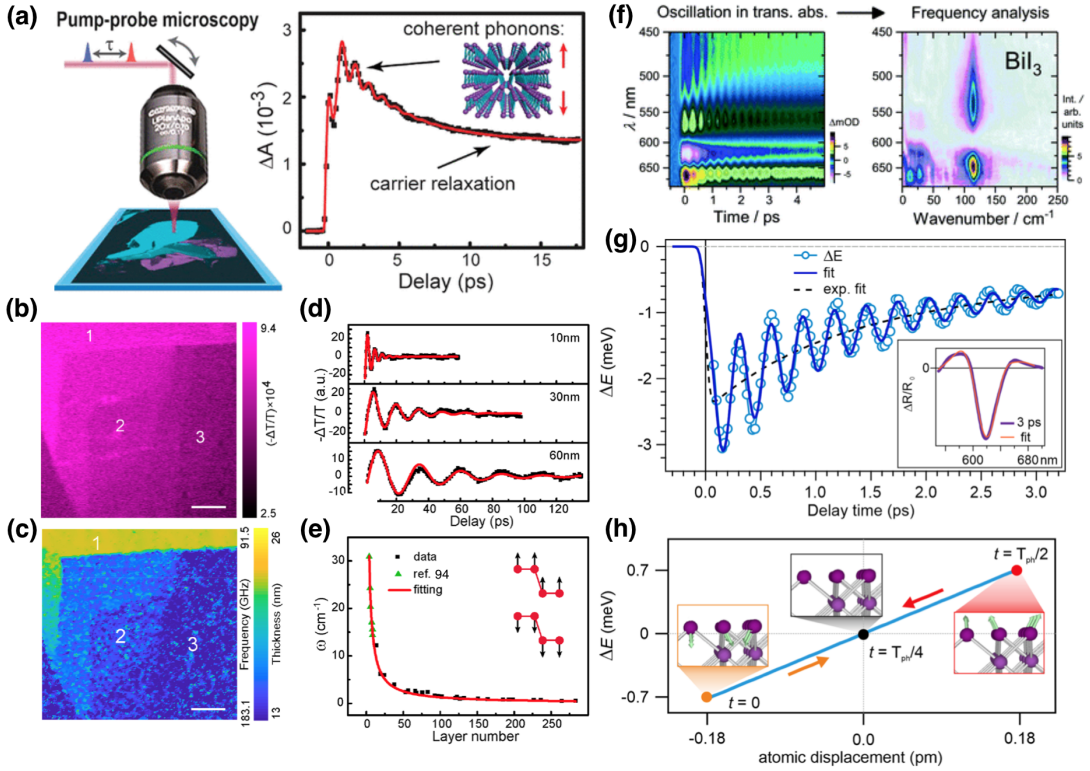

Figure 4. (**a**) Detecting coherent phonon from femtosecond transient absorption microscopy in BP. Copyright 2018, American Chemical Society [108]. (**b**) TA intensity map of a BP flake and (**c**) the corresponding phonon frequency (thickness) distributions. (**d**) Extracted coherent phonon dynamics in 10, 30, and 60 nm thick BP flakes. (**e**) Layer-dependent coherent phonon frequency fitted with the 1D chain model and illustration of the layer-breathing mode. Copyright 2021, American Chemical Society [112]. (**f**) Pronounced coherent A_g oscillations are observed in BiI_3 indicating strong electron-phonon coupling. Copyright 2018, Royal Society of Chemistry [115]. (**g**) Transient energy shift of the excitonic peak in BiI_3, which is obtained by differential fitting of the transient reflectivity spectra after parametrization of the equilibrium reflectance. (**h**) The microscopic effect of exciton-phonon coupling: periodic renormalization of the excitonic peak position by the atomic displacement. Copyright 2021, American Physical Society [116].

5. Conclusions and Outlook

Coherent phonon dynamics in 2D van der Waals semiconductors constitute a pivotal research frontier where quantum control of lattice vibrations enables precise manipulation of electronic, optical, and magnetic properties. As established in Sections 2–4, fundamental generation mechanisms—particularly impulsive stimulated Raman scattering (ISRS) and displacive excitation of coherent phonons (DECP)—have been rigorously verified across diverse material systems (Section 2), with polarization-dependent spectroscopy providing critical discrimination between these pathways. These dynamics, probed through advanced ultrafast spectroscopy (Section 3), govern emergent phenomena in transition metal dichalcogenides (TMDs), magnetic semiconductors, perovskites, and related heterostructures (Section 4). Prospectively, three strategic vectors present exceptional promise: (1) Mechanistic unification via universal frameworks connecting ISRS/DECP dynamics to quantum confinement and interlayer coupling; (2) Cross-dimensional control leveraging phonons to mediate spin-lattice interactions in 2D magnets (Section 4.2) and exciton-phonon coupling in perovskites (Section 4.3); (3) Development of multimodal operando probes integrating spatiotemporal, cryogenic, and stimulus-resolved spectroscopy to decode nonequilibrium energy landscapes. Achieving these goals necessitates prioritizing: unified theoretical frameworks combining first-principles calculations with open quantum system models for coherence lifetime prediction; cryogenic spatiotemporal mapping of interfacial phonon dynamics through combined scanning probe-ultrafast spectroscopy; dynamic phonon engineering via stimulus-tunable spectroscopy; and quantum transduction through coherent magnon-phonon coupling. Collectively, these advances will establish phononics as a foundational discipline enabling energy-efficient excitonic devices exploiting phonon bottlenecks, topologically protected phonon waveguides, and THz-frequency magneto-phononic circuits—paving the way for phonon-coherent quantum technologies with transformative applications in solid-state information processing and energy harvesting.

Author Contributions

X.N.: conceptualization, methodology, data curation, writing—original draft preparation, supervision; J.Z.: writing—reviewing and editing, supervision; X.G.: writing—reviewing and editing, supervision. All authors have read and agreed to the published version of the manuscript.

Funding

This work was supported by the Natural Science Foundation of Jiangsu Province (BK20210276), the Natural Science Foundation of Fujian Province (No. 2024J08081) and Fujian Provincial Educational Scientific Research Project for Middle-aged and Young Teachers (No. JAT231108).

Data Availability Statement

Not applicable.

Conflicts of Interest

The authors declare no conflict of interest.

Use of AI and AI-assisted Technologies

No AI tools were utilized for this paper.

References

1. Cheng, Y.H.; Gao, F.Y.; Teitelbaum, S.W.; et al. Coherent control of optical phonons in bismuth. *Phys. Rev. B* **2017**, *96*, 134302.
2. Liu, S.Y.; Zhu, S.X.; Wu, Q.Y.; et al. Dirac semimetal $PdTe_2$ temperature-dependent quasiparticle dynamics and electron–phonon coupling. *Results Phys.* **2021**, *30*, 104816.
3. Zhu, S.X.; Zhang, C.; Wu, Q.Y.; et al. Temperature evolution of quasiparticle dispersion and dynamics in semimetallic $1T$-$TiTe_2$ via high-resolution angle-resolved photoemission spectroscopy and ultrafast optical pump-probe spectroscopy. *Phys. Rev. B* **2021**, *103*, 115108.
4. Jnawali, J.; Boschetto, D.; Malard, L.M.; et al. Hot carrier transport limits the displacive excitation of coherent phonons in bismuth. *Appl. Phys. Lett.* **2021**, *119*, 091601.
5. Li, Z.; Chen, Y.; Song, A.; et al. Anisotropic phonon dynamics in Dirac semimetal $PtTe_2$ thin films enabled by helicity-dependent ultrafast light excitation. *Light Sci. Appl.* **2024**, *13*, 181.
6. Liu, H.; Zhang, C.; Wu, Q.Y.; et al. Ultrafast photoinduced phase transition in the antiferromagnetic Dirac semimetal EuAgAs. *Phys. Rev. B* **2025**, *111*, L121113.
7. Nakamura, K.G.; Ohya, K.; Takahashi, H.; et al. Spectrally resolved detection in transient-reflectivity measurements of coherent optical phonons in diamond. *Phys. Rev. B* **2016**, *94*, 024303.
8. Hu, J.; Zhang, H.; Sun, Y.; et al. Temperature effect on the coupling between coherent longitudinal phonons and plasmons in n-type and p-type $GaAs$. *Phys. Rev. B* **2018**, *97*, 165307.
9. Werdehausen, D.; Takayama, T.; Höppner, M.; et al. Coherent order parameter oscillations in the ground state of the excitonic insulator Ta_2NiSe_5. *Sci. Adv.* **2018**, *4*, 1734–1738.
10. Bretscher, H.M.; Andrich, P.; Telang, P.; et al. Ultrafast melting and recovery of collective order in the excitonic insulator Ta_2NiSe_5. *Nat. Commun.* **2021**, *12*, 1699.
11. Katsumi, K.; Tsuji, N.; Hamada, Y.I.; et al. Higgs mode in the d-wave superconductor $Bi_2Sr_2CaCu_2O_{8+x}$ driven by an intense terahertz pulse. *Phys. Rev. Lett.* **2018**, *120*, 117001.
12. Zhao, S.Z.; Song, H.Y.; Hu, L.L.; et al. Observation of soft Leggett mode in superconducting $CaKFe_4As_4$. *Phys. Rev. B* **2020**, *102*, 144519.
13. Zhang, C.; Wu, Q.Y.; Hong, W.S.; et al. Ultrafast optical spectroscopy evidence of pseudogap and electron-phonon coupling in an iron-based superconductor $KCa_2Fe_4As_4F_2$. *Sci. China Phys. Mech. Astron.* **2022**, *65*, 237411.
14. Wu, Q.Y.; Zhang, C.; Li, Z.Z.; et al. Hidden nematic fluctuation in the triclinic $(Ca_{0.85}La_{0.15})_{10}(Pt_3As_8)(Fe_2As_2)_5$ superconductor revealed by ultrafast optical spectroscopy. *Phys. Rev. B* **2023**, *108*, 205136.
15. Huang, H.; Zhang, X.; Zhu, J.; et al. Ultrafast charge-transfer dynamics in $Ca_2CuO_2Cl_2$ from time-resolved optical reflectivity. *Phys. Rev. Res.* **2025**, *7*, 023175.
16. Wu, Q.Y.; Zhang, C.; Li, B.Z.; et al. Interplay of electron-phonon coupling, pseudogap, and superconductivity in $CsCa_2Fe_4As_4F_2$ studied using ultrafast optical spectroscopy. *Phys. Rev. B* **2025**, *111*, L081110.
17. Levchuk, A.; Wilk, B.; Vaudel, G.; et al. Coherent acoustic phonons generated by ultrashort terahertz pulses in nanofilms of metals and topological insulators. *Phys. Rev. B* **2020**, *101*, 180102.

18. Wu, Q.; Sun, F.; Zhang, Q.; et al. Quasiparticle dynamics and electron-phonon coupling in Weyl semimetal TaAs. *Phys. Rev. Mater.* **2020**, *4*, 064201.
19. Liu, J.; Cheng, L.; Zhao, D.; et al. Quenching of the relaxation pathway in the Weyl semimetal TaAs. *Phys. Rev. B* **2020**, *102*, 064307.
20. Xu, C.; Zong, A. Time-domain study of coupled collective excitations in quantum materials. *NPJ Quant. Mater.* **2025**, *10*, 21.
21. Kuznetsov, A.V.; Stanton, C.J. Theory of coherent phonon oscillations in semiconductors. *Phys. Rev. Lett.* **1994**, *73*, 3243.
22. Ishioka, K.; Misochko, O.V. Coherent Lattice Oscillations in Solids and Their Optical Control. In *Progress in Ultrafast Intense Laser Science*; Yamanouchi, K., Giulietti, A., Ledingham, K., Eds.; Springer: Berlin/Heidelberg, Germany, 2010; Volume V, pp. 47–63.
23. Dekorsy, T.; Cho, G.C.; Kurz, H. Coherent Lattice Oscillations in Solids and Their Optical Control. In *Light Scattering in Solids VIII 76*; Springer: Berlin/Heidelberg, Germany, 2000; pp. 169–209.
24. Laubereau, A.; Kaiser, W. Vibrational dynamics of liquids and solids investigated by picosecond light pulses. *Rev. Mod. Phys.* **1978**, *50*, 607–665.
25. Shah, J. *Ultrafast Spectroscopy of Semiconductors and Semiconductor Nanostructures*, 2nd ed.; Springer: Berlin, Germany, 1999.
26. Stevens, T.E.; Kuhl, J.; Merlin, R. Coherent phonon generation and the two stimulated Raman tensors. *Phys. Rev. B* **2002**, *65*, 144304.
27. Zeiger, H.J.; Vidal, J.; Cheng, T.K.; et al. Theory for displacive excitation of coherent phonons. *Phys. Rev. B* **1992**, *45*, 768.
28. Garrett, G.A.; Albrecht, T.F.; Whitaker, J.F.; et al. Coherent THz phonons driven by light pulses and the Sb problem: What is the mechanism? *Phys. Rev. Lett.* **1996**, *77*, 3661.
29. Naseska, M.; Sutar, P.; Vengust, D.; Tet al. Orbitally driven insulator-metal transition in $CuIr_2S_4$: Temperature-dependent transient reflectivity study. *Phys. Rev. B* **2020**, *101*, 165134.
30. Zhai, Y.; Gong, P.; Hasaien, J.; et al. Coherent phonons in correlated quantum materials. *Prog. Surf. Sci.* **2024**, *99*, 100761.
31. Yee, K.J.; Lim, Y.S.; Dekorsy, T.; et al. Mechanisms for the generation of coherent longitudinal-optical phonons in GaAs/AlGaAs multiple quantum wells. *Phys. Rev. Lett.* **2001**, *86*, 1630–1633.
32. Basov, D.N.; Averitt, R.D.; van der Marel, D.; et al. Electrodynamics of correlated electron materials. *Rev. Mod. Phys.* **2011**, *83*, 471.
33. Averitt, R.D.; Taylor, A.J. Ultrafast optical and far-infrared quasiparticle dynamics in correlated electron materials. *J. Phys. Condens. Matter* **2002**, *14*, R1357.
34. Sun, C.K.; Vallée, F.; Acioli, L.; et al. Femtosecond investigation of electron thermalization in gold. *Phys. Rev. B* **1993**, *48*, 12365.
35. Demsar, J.; Hudej, R.; Karpinski, J.; et al. Quasiparticle dynamics and gap structure in $HgBa_2Ca_2Cu_3O_{8+\delta}$ investigated with femtosecond spectroscopy. *Phys. Rev. B* **2001**, *63*, 054519.
36. Axt, V.M.; Kuhn, T. Femtosecond spectroscopy in semiconductors: A key to coherences, correlations and quantum kinetics. *Rep. Prog. Phys.* **2004**, *67*, 433.
37. Saida, Y.; Gauthier, T.; Suzuki, H.; et al. Photoinduced dynamics during electronic transfer from narrow to wide bandgap layers in one-dimensional heterostructured materials. *Nat. Commun.* **2024**, *15*, 4600.
38. Wang, Y.; Li, D.; Xing, Z.; et al. Quantum well growth management to smooth the energy transfer pathway for quasi-2D perovskite solar cells. *Adv. Funct. Mater.* **2024**, *34*, 2401203.
39. Gong, A.; Qu, G.; Qiao, Y.; et al. A hot carrier perovskite solar cell with efficiency exceeding 27% enabled by ultrafast hot hole transfer with phthalocyanine derivatives. *Energy Environ. Sci.* **2024**, *17*, 5080.
40. Gao, S.; Xu, S.; Sun, C.; et al. Rational regulation of layer-by-layer processed active layer via trimer-induced pre-swelling strategy for efficient and robust thick-film organic solar cells. *Adv. Mater.* **2025**, *37*, 2420631.
41. Zhang, Q.; Luo, Y. Probing the ultrafast dynamics in nanomaterial complex systems by femtosecond transient absorption spectroscopy. *High Power Laser Sci.* **2016**, *4*, e22.
42. Berera, R.; van Grondelle, R.; Kennis, J.T.M. Ultrafast transient absorption spectroscopy: principles and application to photosynthetic systems. *Photosynth. Res.* **2009**, *101*, 105.
43. Royakkers, J.; Yang, H.; Gillett, A.J.; et al. Synthesis of model heterojunction interfaces reveals molecular-configuration-dependent photoinduced charge transfer. *Nat. Chem.* **2024**, *16*, 1453–1461.
44. Zhang, J.; Zhu, B.; Zhang, L.; et al. Femtosecond transient absorption spectroscopy investigation into the electron transfer mechanism in photocatalysis. *Chem. Commun.* **2023**, *59*, 688.
45. Pan, L.; Dai, L.; Burton, O.J.; et al. High carrier mobility along the [111] orientation in Cu_2O photoelectrodes. *Nature* **2024**, *628*, 765–770.
46. Zewail, A.H. Laser Femtochemistry. *Science* **1988**, *242*, 1645–1653.
47. Fischer, M.P.; Wilson, J.W.; Robles, F.E.; et al. Invited review article: Pump-probe microscopy. *Rev. Sci. Instrum.* **2016**, *87*, 031101.
48. Dong, P.T.; Cheng, J.X. Pump-probe microscopy: Theory, instrumentation, and applications. *Spectroscopy* **2017**, *32*, 24–36.
49. Zhu, Y.; Cheng, J.X. Transient absorption microscopy: Technological innovations and applications in materials science and life science. *J. Chem. Phys.* **2020**, *152*, 020901.

50. Hortensius, J.R.; Afanasiev, D.; Sasani, A.; et al. Ultrafast strain engineering and coherent structural dynamics from resonantly driven optical phonons in $LaAlO_3$. *NPJ Quantum Mater.* **2020**, *5*, 95.
51. de la Torre, A.; Kennes, D.M.; Claassen, M.; et al. Nonthermal pathways to ultrafast control in quantum materials. *Rev. Mod. Phys.* **2021**, *93*, 041002.
52. Henstridge, M.; Först, M.; Rowe, E.; et al. Nonlocal nonlinear phononics. *Nat. Phys.* **2022**, *18*, 457–461.
53. Budden, M.; Gebert, T.; Buzzi, M.; et al. Evidence for metastable photo-induced superconductivity in K_3C_{60}. *Nat. Phys.* **2021**, *17*, 611.
54. Mitrano, M.; Cantaluppi, A.; Nicoletti, D.; et al. Possible light-induced superconductivity in K_3C_{60} at high temperature. *Nature* **2016**, *530*, 461–464.
55. Mankowsky, R.; Först, M.; Cavalleri, A. Non-equilibrium control of complex solids by nonlinear phononics. *Rep. Prog. Phys.* **2016**, *79*, 064503.
56. Mankowsky, R.; Subedi, A.; Först, M.; et al. Nonlinear lattice dynamics as a basis for enhanced superconductivity in $YBa_2Cu_3O_{6.5}$. *Nature* **2014**, *516*, 71.
57. Fausti, D.; Tobey, R.I.; Dean, N.; et al. Light-induced superconductivity in a stripe-ordered cuprate. *Science* **2011**, *331*, 189.
58. Marciniak, A.; Marcantoni, S.; Giusti, F.; et al. Vibrational coherent control of localized d–d electronic excitation. *Nat. Phys.* **2021**, *17*, 368–373.
59. Zalalutdinov, M.K.; Robinson, J.T.; Fonseca, J.J.; et al. Acoustic cavities in 2D heterostructures. *Nat. Commun.* **2021**, *12*, 3267.
60. Mankowsky, R.; von Hoegen, A.; Först, M.; et al. Ultrafast reversal of the ferroelectric polarization. *Phys. Rev. Lett.* **2017**, *118*, 197601.
61. Nova, T.; Disa, A.; Fechner, M.; et al. Metastable ferroelectricity in optically strained $SrTiO_3$. *Science* **2019**, *364*, 1075–1079.
62. Li, X.; Qiu, T.; Zhang, J.; et al. Terahertz field–induced ferroelectricity in quantum paraelectric $SrTiO_2$. *Science* **2019**, *364*, 1079–1082.
63. Zhang, Y.; Dai, J.; Zhong, X.; et al. Probing ultrafast dynamics of ferroelectrics by time-resolved pump-probe spectroscopy. *Adv. Sci.* **2021**, *8*, 2102488.
64. Afanasiev, D.; Hortensius, J.R.; Ivanov, B.A.; et al. Ultrafast control of magnetic interactions via light-driven phonons. *Nat. Mater.* **2021**, *20*, 607–611.
65. Stupakiewicz, A.; Davies, C.S.; Szerenos, K.; et al. Ultrafast phononic switching of magnetization. *Nat. Phys.* **2021**, *17*, 489–492.
66. Bae, Y.J.; Wang, J.; Scheie, A.; et al. Exciton-coupled coherent magnons in a 2D semiconductor. *Nature* **2022**, *609*, 282–286.
67. Ergeçen, E.; Ilyas, B.; Kim, J.; et al. Coherent detection of hidden spin–lattice coupling in a van der Waals antiferromagnet. *Proc. Natl. Acad. Sci. USA* **2023**, *120*, e2208968120.
68. Lopez, D.A.B.; Juraschek, D.M.; Fechner, M.; et al. Ultrafast simultaneous manipulation of multiple ferroic orders through nonlinear phonon excitation. *NPJ Quant. Mater.* **2025**, *10*, 24.
69. Rini, M.; Tobey, R.; Dean, N.; et al. Control of the electronic phase of a manganite by mode-selective vibrational excitation. *Nature* **2007**, *449*, 72–74.
70. Cocker, T.L.; Titova, L.V.; Fourmaux, S.; et al. Phase diagram of the ultrafast photoinduced insulator-metal transition in vanadium dioxide. *Phys. Rev. B* **2012**, *85*, 155120.
71. Guan, M.; Chen, D.; Chen, Q.; et al. Coherent phonon assisted ultrafast order-parameter reversal and hidden metallic state in Ta_2NiSe_5. *Phys. Rev. Lett.* **2023**, *131*, 256503.
72. Liu, Q.M.; Wu, D.; Li, Z.A.; et al. Photoinduced multistage phase transitions in Ta_2NiSe_5. *Nat. Commun.* **2021**, *12*, 2050.
73. Kirby, R.J.; Muechler, L.; Klemenz, S.; et al. Signature of an ultrafast photoinduced Lifshitz transition in the nodal-line semimetal ZrSiTe. *Phys. Rev. B* **2021**, *103*, 205138.
74. Carr, A.D.; Ruppert, C.; Samusev, A.K.; et al. Enhanced photon-phonon interaction in WSe_2 acoustic nanocavities. *ACS Photonics* **2024**, *11*, 1147–1155.
75. Li, C.; Scherbakov, A.V.; Soubelet, P.; et al. Coherent phonons in van der Waals $MoSe_2/WSe_2$ heterobilayers. *Nano Lett.* **2023**, *23*, 8186–8193.
76. Soubelet, P.; Reynoso, A.A.; Fainstein, A.; et al. The lifetime of interlayer breathing modes of few-layer $2H - MoSe_2$ membranes. *Nanoscale* **2019**, *11*, 10446–10453.
77. Koshihara, S.; Tokura, Y.; Mitani, T.; et al. Photoinduced valence instability in the organic molecular compound tetrathiafulvalene-p-chloranil (TTF-CA). *Phys. Rev. B* **1990**, *42*, 6853–6856.
78. Tian, Y.C.; Zhang, W.H.; Li, F.S.; et al. Ultrafast dynamics evidence of high temperature superconductivity in single unit cell FeSe on $SrTiO_3$. *Phys. Rev. Lett* **2016**, *116*, 107001.
79. Gerber, S.; Yang, S.L.; Zhu, D.; et al. Femtosecond electron-phonon lock-in by photoemission and X-ray free-electron laser. *Science* **2017**, *357*, 71–75.
80. Wu, Q.; Zhou, H.; Wu, Y.; et al. Ultrafast quasiparticle dynamics and electron-phonon coupling in $(Li_{0.84}Fe_{0.16})OH\,Fe_{0.98}Se$. *Chin. Phys. Lett.* **2020**, *37*, 097802.

81. Stojchevska, L.; Vaskivskyi, I.; Mertelj, T.; et al. Ultrafast switching to a stable hidden quantum state in an electronic crystal. *Science* **2014**, *344*, 177–180.
82. Hasaien, J.; Wu, Y.; Shi, M.; et al. Emergent quantum state unveiled by ultrafast collective dynamics in $1T$-TaS_2. *Proc. Natl. Acad. Sci. USA* **2025**, *122*, e2406464122.
83. Först, M.; Manzoni, C.; Kaiser, S.; et al. Nonlinear phononics as an ultrafast route to lattice control. *Nat. Phys.* **2011**, *7*, 854.
84. Wang, Y.H.; Steinberg, H.; Jarillo-Herrero, P.; et al. Observation of floquet-bloch states on the surface of a topological insulator. *Science* **2013**, *342*, 453–457.
85. McIver, J.W.; Schulte, B.; Stein, F.U.; et al. Light-induced anomalous hall effect in graphene. *Nat. Phys.* **2020**, *16*, 38–41.
86. Jeong, T.Y.; Jin, B.M.; Rhim, S.H.; et al. Coherent lattice vibrations in mono- and few-layer WSe_2. *ACS Nano* **2016**, *10*, 5560.
87. Sayers, C.J.; Genco, A.; Trovatello, C.; et al. Strong coupling of coherent phonons to excitons in semiconducting monolayer $MoTe_2$. *Nano Lett.* **2023**, *23*, 9235–9242.
88. Trovatello, C.; Miranda, H.P.C.; Molina-Sánchez, A.; et al. Strongly coupled coherent phonons in single-layer MoS_2. *ACS Nano* **2020**, *14*, 5700–5710.
89. Yang, J.; Xie, J.; Jiang, S.; et al. Extraordinary polarization and thickness dependences of photocarrier dynamics in $PdSe_2$ ribbons. *J. Phys. Chem. Lett.* **2024**, *15*, 4276–4285.
90. Lyu, X.; Li, Y.; Li, X.; et al. Layer-dependent ultrafast carrier dynamics of $PdSe_2$ investigated by photoemission electron microscopy. *Nanoscale* **2024**, *16*, 9317–9324.
91. Huo, C.F.; Wen, R.; Yan, X.Q.; et al. Thickness-dependent ultrafast charge-carrier dynamics and coherent acoustic phonon oscillations in mechanically exfoliated $PdSe_2$ flakes. *Phys. Chem. Chem. Phys.* **2021**, *23*, 20666–20674.
92. Chen, X.; Zhang, S.; Wang, L.; et al. Direct observation of interlayer coherent acoustic phonon dynamics in bilayer and few-layer $PdSe_2$. *Photon. Res.* **2019**, *7*, 1416–1424.
93. Suo, P.; Yan, S.; Pu, R.; et al. Ultrafast photocarrier and coherent phonon dynamics in type-II Dirac semimetal $PtTe_2$ thin films probed by optical spectroscopy. *Photon. Res.* **2022**, *10*, 653–661.
94. Belvin, C.A.; Baldini, E.; Ozel, I.O.; et al. Exciton-driven antiferromagnetic metal in a correlated van der Waals insulator. *Nat. Commun.* **2021**, *12*, 4837.
95. Dirnberger, F.; Quan, J.; Bushati, R.; et al. Magneto-optics in a van der Waals magnet tuned by self-hybridized polaritons. *Nature* **2023**, *620*, 533–537.
96. Wilson, N.P.; Lee, K.; Cenker, J.; et al. Interlayer electronic coupling on demand in a 2D magnetic semiconductor. *Nat. Mater.* **2021**, *20*, 1657–1662.
97. Wu, J.B.; Wu, H.; Tan, P.H. Magneto-optical interactions in layered magnets. *Adv. Funct. Mater.* **2024**, *2024*, 2312214.
98. Lloyd-Hughes, J.; Oppeneer, P.M.; Pereira dos Santos, T.; et al. The 2021 ultrafast spectroscopic probes of condensed matter roadmap. *J. Phys. Condens. Matter* **2021**, *33*, 353001.
99. Gong, S.; Huang, Y.; Yu, X.; et al. Ultrafast dynamics in perovskite-based optoelectronic devices. *Cell Rep. Phys. Sci.* **2023**, *4*, 101580.
100. Fu, J.; Xu, Q.; Han, G.; et al. Hot carrier cooling mechanisms in halide perovskites. *Nat. Commun.* **2017**, *8*, 1300.
101. Yang, Y.; Ostrowski, D.P.; France, R.M.; et al. Observation of a hot-phonon bottleneck in lead-iodide perovskites. *Nat. Photonics* **2016**, *10*, 53–59.
102. Thouin, F.; Valverde-Chávez, D.A.; Quarti, C.; et al. Phonon coherences reveal the polaronic character of excitons in two-dimensional lead halide perovskites. *Nat. Mater.* **2019**, *18*, 349–356.
103. Seyitliyev, D.; Qin, X.; Jana, M.K.; et al. Coherent phonon-induced modulation of charge transfer in 2D hybrid perovskites. *Adv. Funct. Mater.* **2023**, *33*, 2213021.
104. Guo, P.; Stoumpos, C.C.; Mao, L.; et al. Cross-plane coherent acoustic phonons in two-dimensional organic-inorganic hybrid perovskites. *Nat. Commun.* **2018**, *9*, 2019.
105. Maity, P.; Yin, J.; Cheng, B.; et al. Layer-dependent coherent acoustic phonons in two-dimensional ruddlesden-popper perovskite crystals. *J. Phys. Chem. Lett.* **2019**, *10*, 5259–5264.
106. Quan, L.N.; Park, Y.; Guo, P.; et al. Vibrational relaxation dynamics in layered perovskite quantum wells. *Proc. Natl. Acad. Sci. USA* **2021**, *118*, e2104425118.
107. Cui, M.; Qin, C.; Zhou, Z.; et al. Tuning coherent phonon dynamics in two-dimensional phenylethylammonium lead bromide perovskites. *Nano Res.* **2023**, *16*, 3408–3414.
108. Miao, X.; Zhang, G.; Wang, F.; et al. Layer-dependent ultrafast carrier and coherent phonon dynamics in black phosphorus. *Nano Lett.* **2018**, *18*, 3053–3059.
109. Xia, F.; Wang, H.; Jia, Y. Rediscovering black phosphorus as an anisotropic layered material for optoelectronics and electronics. *Nat. Commun.* **2014**, *5*, 4458.
110. Ge, S.; Li, C.; Zhang, Z.; et al. Dynamical evolution of anisotropic response in black phosphorus under ultrafast photoexcitation. *Nano Lett.* **2015**, *15*, 4650–4656.
111. Meng, S.; Shi, H.; Jiang, H.; et al. Anisotropic charge carrier and coherent acoustic phonon dynamics of black phosphorus studied by transient absorption microscopy. *J. Phys. Chem. C* **2019**, *123*, 20051–20058.

112. Wu, S.; Lu, Z.; Hu, A.; et al. Dichroic photoelasticity in black phosphorus revealed by ultrafast coherent phonon dynamics. *J. Phys. Chem. Lett.* **2021**, *12*, 5871–5878.
113. Chebl, M.; He, X.; Yang, D.S. Ultrafast carrier-coupled interlayer contraction, coherent intralayer motions, and phonon thermalization dynamics of black phosphorus. *Nano Lett.* **2022**, *22*, 5230–5235.
114. Wu, S.; Chu, W.; Lu, Y.; et al. Imaging ultrafast dynamics of pressure-driven phase transitions in black phosphorus and anomalous coherent phonon softening. *Nano Lett.* **2024**, *24*, 424–432.
115. Scholz, M.; Oum, K.; Lenzer, T. Pronounced exciton and coherent phonon dynamics in BiI_3. *Phys. Chem. Chem. Phys.* **2018**, *20*, 10677.
116. Mor, S.; Gosetti, V.; Molina-Sánchez, A.; et al. Photoinduced modulation of the excitonic resonance via coupling with coherent phonons in a layered semiconductor. *Phys. Rev. Res.* **2021**, *3*, 043175.